The structural proteins of epidemic and historical strains of Zika virus differ in their ability to initiate viral infection in human host cells

Sandra Bos, Wildriss Viranaicken, Jonathan Turpin, Chaker El Kalamouni, Marjolaine Roche, Pascale Krejbich-Trotot, Philippe Desprès, Gilles Gadea

HAL Id: hal-01702657

https://hal.univ-reunion.fr/hal-01702657v1

Submitted on 14 Nov 2020

The structural proteins of epidemic and historical strains of Zika virus differ in their ability to initiate viral infection in human host cells

Sandra Bos, Wildriss Viranaicken, Jonathan Turpin, Chaker El-Kalamouni, Marjolaine Roche, Pascale Krejbich-Trotot, Philippe Desprès*, Gilles Gadea*

Université de la Réunion, INSERM U1187, CNRS UMR 9192, IRD UMR 249, Unité Mixte Processus Infectieux en Milieu Insulaire Tropical, Plateforme Technologique CYROI, 94791 Sainte Clotilde, La Réunion, France

ARTICLE INFO

ABSTRACT

Mosquito-borne Zika virus (ZIKV) recently emerged in South Pacific islands and Americas where large epidemics were documented. In the present study, we investigated the contribution of the structural proteins C, prM and E in the permissiveness of human host cells to epidemic strains of ZIKV. To this end, we evaluated the capacity of the epidemic strain BeH819015 to infect epithelial A549 and neuronal SH-SY5Y cells in comparison to the African historical MR766 strain. For that purpose, we generated a molecular clone of BeH819015 and a chimeric clone of MR766 which contains the BeH819015 structural protein region. We showed that ZIKV containing BeH819015 structural proteins was much less efficient in cell-attachment leading to a reduced susceptibility of A549 and SH-SY5Y cells to viral infection. Our data illustrate a previously underrated role for C, prM, and E in ZIKV epidemic strain ability to initiate viral infection in human host cells.

1. Introduction

Zika virus (ZIKV) is an emerging mosquito-borne *flavivirus* (*Flaviviridae* family) that became a major medical concern worldwide. In 2007, the first ZIKV epidemic occurred in the Yap Island affecting more than 70% of the inhabitants (Duffy et al., 2009). Subsequently, ZIKV continued to spread in the South Pacific islands and widely emerged in the Americas from 2015 (Gatherer and Kohl, 2016). Phylogenetic analysis of viral sequences identified the African and Asian genotypes of ZIKV (Haddow et al., 2012), the Asiatic strains being the leading cause of the major current epidemics with millions of infection cases (Giovanetti et al., 2016). While a large majority of infections caused by ZIKV are asymptomatic, or result in dengue-like symptoms, epidemiological studies have pointed out that ZIKV infection can also cause severe diseases in humans including Guillain-Barre syndrome and congenital neurological defects (microcephaly) (Cao-Lormeau et al., 2016; Cugola et al., 2016; Merfeld et al., 2017; Parra et al., 2016). Unlike most other flaviviruses, a component of the spread of ZIKV may reflect its potential for human-to-human transmission. ZIKV is believed to disseminate using both sexual and non-sexual routes including body fluids such as tears, saliva or blood (D'Ortenzio et al., 2016; Motta et al., 2016; Musso et al., 2016). The risk of human infection by solid organ transplantation has also been suggested (Alcendor, 2017).

ZIKV contains a single-strand positive sense genomic RNA, which is translated into a large and unique polyprotein. The polyprotein is then processed by host and viral proteases into three structural proteins (C, prM/M and E), and seven nonstructural (NS) proteins (NS1 to NS5). Recently, we reported the generation of an infectious cDNA clone of MR766 (hereafter MR766[MC]) based on the GenBank access number LC002520 (MR766-NIID) after electroporation of four overlapping synthetic fragments that cover the genomic RNA sequence using the ISA method (Atieh et al., 2016; Gadea et al., 2016). The African historical ZIKV strain MR766 was initially collected from a rhesus monkey in Uganda in 1947 and serially propagated in new-born mouse brains (Dick et al., 1952). It is not known whether the mouse neuroadaptation of MR766 resulted in accumulation of mutations in viral sequence.

Epidemic strains of ZIKV have the capacity to replicate in diverse cell types of human origin including epithelial and neuronal cells (Hamel et al., 2017; Pagani et al., 2017; Sheridan et al., 2017; Simonin et al., 2016; Tripathi et al., 2017). We reported that infection of human lung epithelial A549 cells with ZIKV strain PF-25013-18 of Asian lineage isolated during the epidemic in French Polynesia in 2013 (Cao-Lormeau et al., 2014; Frumence et al., 2016) resulted in the activation of Interferon Stimulated Genes (ISGs), the production of Type-I

---

* Corresponding authors.
E-mail addresses: philippe.despres@univ-reunion.fr (P. Desprès), gilles.gadea@inserm.fr (G. Gadea).

interferon (IFN) associated to expression of pro-inflammatory cytokines, and induction of apoptosis. Several reports highlighted the preponderant role of the NS proteins in the responsiveness of human host cells to ZIKV infection. Here, we studied the role of the structural proteins in the permissiveness of human neuroblastoma SH-SY5Y and A549 cells to infection with epidemic strains of ZIKV. Using the ISA method, we generated a molecular clone of ZIKV strain BeH819015 isolated from a human serum specimen in Brazil in 2015 and a chimeric clone of MR766 in which the structural protein region was replaced with the one of BeH819015. Comparative analysis between the three viral clones revealed that ZIKV containing BeH819015 structural proteins are less efficient in the initiation of viral infection in human cells when compared to MR766^{MC}.

2. Methods

2.1. Cells and reagents

Vero cells (ATCC, CCL-81) were cultured at 37 °C under a 5% CO2 atmosphere in MEM medium, supplemented with 5% heat-inactivated foetal bovine serum (FBS), A549-Dual™ cells (InvivoGen, a549d-nfis) designated hereafter as A549^{DUAL} cells and SH-SY5Y cells (ATCC, CRL2266) in MEM medium, supplemented with 10% heat-inactivated FBS and non-essential amino acids. A549-Dual™ (A549^{Dual}) cells were maintained in growth medium supplemented with 10 μg mL^{-1} blasticidin and 100 mg mL^{-1} zeocin (InvivoGen). The mouse anti-pan flavivirus envelope E protein mAb 4G2 was produced by RD Biotech. The rabbit anti-BAX and anti-caspase 3 antibodies were purchased from Cell Signalling Technology, the anti-cleaved PARP antibody from Promega, donkey anti-mouse Alexa Fluor 488 and anti-rabbit Alexa Fluor 594 IgG antibodies from Invitrogen. Horseradish peroxidase-conjugated anti-rabbit and anti-mouse antibodies were purchased from Vector Labs.

2.2. Design of ZIKV molecular clones

The molecular clone design and production strategies for ZIKV were previously described by Gadea et al. (2016). The viral clone BR15^{MC} was produced as described for MR766^{MC} (Gadea et al., 2016). BR15^{MC} was based on the sequence of epidemic ZIKV strain BeH819015 (GenBank access KU365778) isolated in Brazil in 2015. MR766 was passaged more than hundred times in new-born mouse brain, and BeH819015 was isolated from blood patient and sequenced after one passage on C6/36 (Dick et al., 1952; Faria et al., 2016). Because the sequences of the untranslated regions (UTRs) deposited in GenBank were partial and also showed abnormalities, the 5'UTR of MR766^{MC} and the 3'UTR of contemporary clinical isolate Paraiba of ZIKV (GenBank access KX280026) were chosen to generate BR15^{MC}. The 3'UTRs from BR15^{MC} and MR766^{MC} perfectly matched on the last 150 nucleotides. Based on our previous experience with molecular clone of ZIKV that used overlapping PCR products (Gadea et al., 2016), the design of viral genome into four viral genomic fragments Z1^{BR15}, Z2^{BR15}, Z3^{BR15} and Z4^{BR15} was chosen to mimic those used to construct MR766^{MC}. The fragment Z1^{BR15} contains the CMV promoter immediately adjacent to the 5'UTR of ZIKV followed by the structural protein region of strain BeH819015. Two synonymous mutations at positions 2200 (a - > g) and 2215 (t - > c) of the structural protein region of ZIKV strain BeH819015 were introduced for a perfect matching of the fragments Z1^{BR15} and Z2$^{NIID-MC}$ on 42 nucleotides. A silent mutation in the E gene that creates the unique restriction site *Pvu* I was introduced into the Z1^{BR15} fragment. The fragment Z4^{BR15} consists of a hepatitis delta virus ribozyme immediately following the last ZIKV nucleotide and a SV40 poly(A) signal. The synthetic genes Z1^{BR15}, Z2^{BR15}, Z3^{BR15}, and Z4^{BR15} were synthesized and cloned into plasmid pUC57 by GeneCust (Luxembourg). The fragments Z1^{BR15} to Z4^{BR15} were amplified by PCR from their respective plasmids using a set of primer pairs that were designed so that Z1^{BR15} and Z2^{BR15} or Z3^{BR15} and Z4^{BR15} matched on about

30–40 nucleotides.

2.3. Recovering of molecular clone BR15^{MC} and chimeric virus CHIM

The molecular clone BR15^{MC} was produced as previously described for MR766^{MC}. Briefly, the purified PCR fragments Z1^{BR15}, Z2^{BR15}, Z3^{BR15}, and Z4^{BR15} were electroporated into Vero cells. After 5 days, cell supernatants were recovered and used to infect fresh Vero cells in a first round of amplification (P1). Viral clone BR15^{MC} was recovered 7 days later and amplified for another 2 days on Vero cells to produce a P2 for further studies. The viral clone BR15^{MC} derived from ZIKV strain BeH819015 is available to BEI Resources (Manassas, VA) under the catalog number NR-51129 (www.beiresources.org). To produce the viral clone CHIM, Vero cells were electroporated with the PCR fragments Z1^{BR15}, Z2$^{MR766-MC}$, Z3$^{MR766-MC}$, and Z4$^{MR766-MC}$. The recovered virus CHIM consists of the viral sequence of MR766 in which the coding region for the structural proteins was replaced with the counterpart of ZIKV strain BeH819015. The viral clone CHIM contains a chimeric E protein between BeH819015 (amino acids 1–436) and MR766 (amino acids 437–504).

2.4. Plaque forming assay

Viral titers were determined by a standard plaque-forming assay as previously described with minor modifications (Frumence et al., 2016). Briefly, Vero cells grown in 48-well culture plate were infected with tenfold dilutions of virus samples for 2 h at 37 °C and then incubated with 0.8% carboxymethylcellulose (CMC) for 4 days. The cells were fixed by 3.7% FA in PBS and stained with 0.5% crystal violet in 20% ethanol. Viral titers were expressed as plaque-forming units per mL (PFU.mL^{-1}).

2.5. Quantification of viral stocks

Zika virus samples were analyzed by titration on Vero cells while genomic viral RNA was quantified by RT-qPCR. For viral genome quantification, viral RNA was extracted from virus particles using QIAmp kit (QIAGEN). The PCR standard curve used for the quantification of ZIKV copy numbers was obtained with a pUC57/ZIKV-E amplicon plasmid containing a synthetic cDNA encompassing nucleotides 961–1301 of genomic RNA (GenBank accession number LC002520). The couple of ZIKV E primers was used to equally amplify pUC57/ZIKV-E amplicon and the cDNA encompassing nucleotides 1046–1213 from genomic RNA of ZIKV molecular clones used in this study.

2.6. Immunoblot assay

Cell lysates were performed in RIPA lysis buffer. All subsequent steps of immunoblotting was performed as described (Nativel et al., 2013; Viranaicken et al., 2011). Primary antibodies were used at 1:500 dilutions. Anti-rabbit immunoglobulin-horseradish peroxidase and anti-mouse immunoglobulin-horseradish peroxidase conjugates were used as secondary antibodies (dilution 1:2000). Blots were revealed with ECL detection reagents. Bands were quantified by densitometry using ImageJ software.

2.7. Immunofluorescence assay

A549^{Dual} cells grown on glass coverslips were fixed with 3.7% formaldehyde at room temperature for 10 min. Fixed were permeabilized with 0.1% Triton X-100 in PBS for 4 min. Cells were stained using the mouse anti-pan flavivirus envelope E protein mAb 4G2 (1:1000 dilution), rabbit anti-Caspase 3 mAb (1:1000 dilution) and rabbit anti-BAX mAb (1:1000 dilution). Antigen staining was visualized with Alexa Fluor-conjugated class specific secondary antibodies (1:1000, Invitrogen). Nucleus morphology was revealed by DAPI staining. The

coverslips were mounted with VECTASHIELD® (VECTOR Laboratories), and fluorescence was observed using a Nikon Eclipse E2000-U microscope. Images were captured and processed using a Hamamatsu ORCA-ER camera and the imaging software NIS-Element AR (Nikon).

2.8. Flow cytometry assay

A549^{Dual} cells were grown on 6-well plates at 5.10^5 cells per well and infected at a multiplicity of infection (MOI) of 1. Infected cells were harvested and fixed with 3.7% formaldehyde in PBS for 20 min, permeabilized with 0.1% Triton-X100 in PBS for 4 min and then blocked with PBS-BSA for 10 min. Cells were stained with anti-E 4G2 (1:1000) for 1 h. Antigen staining was visualized with goat anti-mouse Alexa Fluor 488 IgG (1:1000) for 20 min. Cells were subjected to a flow cytometric analysis using FACScan flow cytometer (BD Bioscience). The percentage of positive cells was determined using FlowJo software.

2.9. RT-qPCR

Total RNA including genomic viral RNA was extracted from cells (Qiagen) and reverse transcription was performed using 500 ng of total RNA, random hexamer primers (intracellular viral RNA) or E reverse primer (virus particles) and MMLV reverse transcriptase (Life Technologies) at 42 °C for 50 min. Quantitative PCR was performed on a ABI7500 Real-Time PCR System (Applied Biosystems). Briefly, 10 ng cDNA was amplified using 0.2 μM of each primer and 1X GoTaq Master Mix (Promega). When appropriate, data were normalized to the internal standard GAPDH. For each single-well amplification reaction, a threshold cycle (Ct) was calculated using the ABI7500 program (Applied Biosystems) in the exponential phase of amplification. Relative changes in gene expression were determined using the 2ΔΔCt method and reported relative to the control. The primers used in this study are listed in Frumence et al. (2016). ZIKV E primers were designed to match both MR766-NIID and BeH819015 sequences (forward 5-gtcttggaacatggagg-3' and reverse 5'-ttcaccttgtgttgggc-3').

2.10. Virus binding assay

Cells were cultured at subconfluent density in 60 mm dishes. Cell monolayers were washed in cold PBS and cooled at 4 °c at least 20 min in presence of cold MEM supplemented with 2% FBS. Pre-chilled cells were incubated at 4 °C with ZIKV at MOI of 1 (A549^{Dual} cells) or 10 (SH-SY5Y cells) in 1.5 or 3.0 mL of cold MEM supplemented with 2% FBS. After 1 h of incubation, the virus inputs were removed and the cells were washed with cold MEM supplemented with 2% FBS. Total cellular RNA was extracted using the RNeasy kit (Qiagen) and RT-qPCR analysis on viral RNA was performed using primers for ZIKV E gene as above described.

2.11. Cytotoxicity assay

Cell damages were evaluated measuring lactate dehydrogenase (LDH) release. Supernatants of infected cells were recovered and subjected to a cytotoxicity assay, performed using CytoTox 96® non-radioactive cytotoxicity assay (Promega) according to manufacturer instructions. Absorbance of converted dye was measured at 490 nm (Tecan). Results of LDH activity are presented with subtraction of control values.

2.12. NF-κB and IFN-β pathway activation

The activation of the NF-κB and IRF pathways were monitored measuring the SEAP and *Lucia* luciferase activities, respectively. The SEAP activity was evaluated using the QUANTI-blue substrate (InvivoGen) according to the manufacturer's instructions. NF-κB-induced SEAP levels were quantified using a microplate spectrophotometer at 620 nm (TECAN). The *Lucia* luciferase activity was evaluated using the QUANTI-Luc substrate (InvivoGen) according to the manufacturer's recommendations. IRF-induced luciferase levels were quantified using a FLUOstar Omega Microplate Reader (BMG LABTECH). Results are presented with subtraction of control values.

2.13. Statistical analysis

All values are expressed as mean ± SD of at least two experiments, or as mean ± SEM of triplicates. Comparisons between different treatments have been analyzed by a one-way or two-way ANOVA tests as appropriate. Values of $p < 0.05$ were considered statistically significant for a post-hoc Tukey's test. All statistical tests were done using the software Graph-Pad Prism version 7.01.

3. Results

3.1. Characterization of viral clones

In an effort to better understand the role of C, prM, and E in the permissiveness of human cells to ZIKV infection, we generated the molecular clones BR15^{MC} based on the sequence of the ZIKV strain BeH819015 and CHIM, a chimera derived from MR766^{MC} in which the structural protein region of MR766 was replaced with the one of BeH819015 (Fig. 1A). BR15^{MC} and CHIM sequence design into four overlapping large fragments was chosen to mimic those initially used to generate MR766^{MC} using the ISA method (Gadea et al., 2016). The chimeric MR766, referred as CHIM, had the 5' and 3'-UTR sequences and the nonstructural proteins coding sequence of MR766, and the structural proteins C-1 to E-436 derived from BeH819015. The genomes of BR15^{MC} and CHIM were assembled in Vero cells by electroporation of the four overlapping fragments corresponding to the full-length genomic RNA. The viruses recovered in the cell supernatants were twice amplified on Vero cells. The titers of viral stocks P2 were determined on Vero cells (Table 1). We noted that BR15^{MC} generated plaques on Vero cells of smaller size than MR766^{MC} or CHIM (Fig. 1B). Also, BR15^{MC} stock had a lower infectious titer than MR766^{MC} and CHIM stocks. There was a constant infectivity ratio of about 1000 viral RNA copies/PFU regardless viral clones (Table 1). Accordingly, the viral stocks P2 of MR766^{MC}, BR15^{MC} and CHIM were suitable for further comparative analysis.

3.2. Susceptibility of A549 and SH-SY5Y cells to viral clones

The study of ZIKV progeny production in A549^{Dual} cells infected with viral clones at MOI of 1 showed that BR15^{MC} and CHIM replicated more slowly than MR766^{MC} (Fig. 2A). A such delay in viral growth was corroborated with the percentage of positive cells determined by FACS assay as well as rate of intracellular viral RNA at early infection times (Fig. 3). In SH-SY5Y cells infected with BR15^{MC} or CHIM at MOI of 10, progeny production of both viral clones was reduced at, at least, 3 log when compared to MR766^{MC} at viral growth plateau (Fig. 2A). Thus, ZIKV containing BeH819015 structural proteins were less efficient in their capacity to infect A549^{Dual} and SH-SY5Y cells when compared to African strain.

The attachment of virus particles to cell surface is a pre-requisite for the initiation of ZIKV infection in the host cells. Virus binding assays were performed to determine whether the lower capacity of BR15^{MC} and CHIM to infect human host cells was due to a difference in cell-attachment (Fig. 2B). A549^{Dual} and SH-SY5Y cells were incubated with viral clones and virus particles binding was evaluated by RT-qPCR. A reduction of at least 80% of BR15^{MC} and CHIM binding was observed compared to MR766^{MC} regardless of the human cell lines tested. Thus, ZIKV containing BeH819015 structural proteins significantly differed from MR766 in their capacity to initiate viral infection in A549^{Dual} and SH-SY5Y cells. These results suggested that permissiveness of human
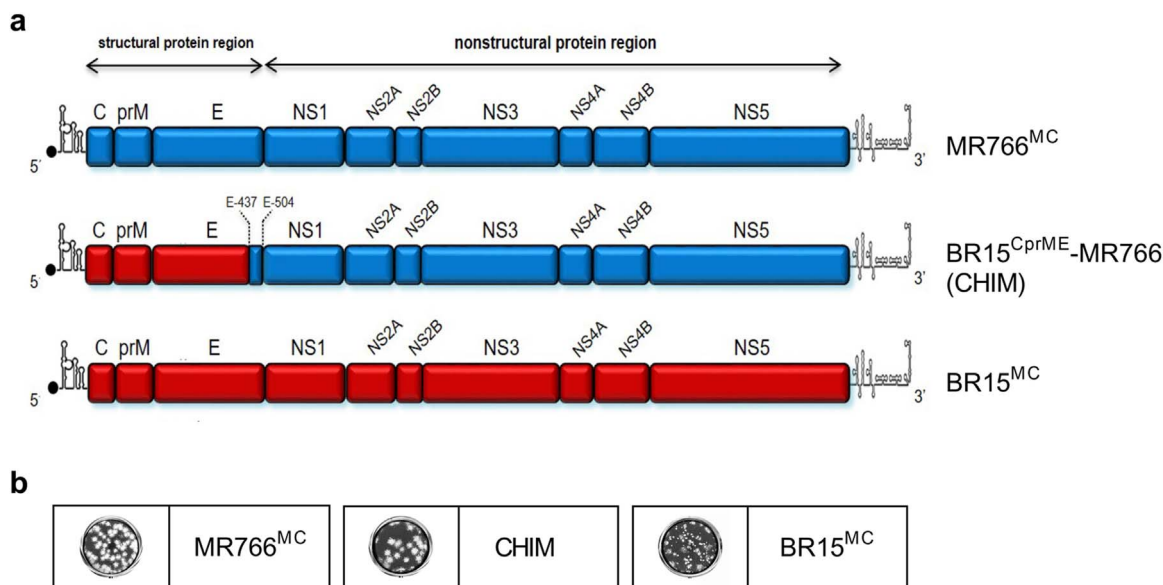
Fig. 1. ZIKV molecular clones MR766, BR15 and CHIM. *In* (A), schematic representation of viral clone BR15[MC] derived from ZIKV strain BeH819015 and MR766[MC] which had been described elsewhere (Gadea et al., 2016). The chimeric clone CHIM expresses most of the structural proteins (C, prM, and E [amino acid sequence 1–436]) of BeH819015 fused to part of the E protein (amino acids 437–504) and the non-structural proteins (NS1 to NS5) of MR766[MC]. *In* (B), examples of infectious plaques developed for MR766[MC], BR15[MC], and CHIM, after plaque forming assay on Vero cells.

Table 1
Infectivity of viral clones.

Virus stocks	vRNA copies.mL^{-1}	PFU.mL^{-1}	Ratio[a]
MR766[MC]	5.3×10^{10}	5×10^{7}	1008
CHIM	2.3×10^{10}	2×10^{7}	1084
BR15[MC]	4.5×10^{9}	5×10^{6}	853

[a] Viral RNA copies/PFU ratio was determined for each virus stock P2 produced in Vero cells by dividing the number viral RNA copies as measured by RT-qPCR with the number of PFU determined in Vero cells.

cells to ZIKV infection is related, in part, to the binding efficacy of viral structural proteins to host cell membrane.

3.3. Apoptosis in A549 cells infected with viral clones

Given that BR15[MC] and CHIM reached a plateau of virus progeny production in A549[Dual] cells 24 h later than M766[MC] (Fig. 2A), we assessed whether this delay in viral growth was associated with variations in host-cell responses to ZIKV infection. Analysis of LDH release in A549[Dual] cells infected 48 h with ZIKV revealed a severe loss of cell integrity in response to MR766[MC] infection but not to BR15[MC] and CHIM (Fig. 4A). Thus, the viability of A549[Dual] cells infected with ZIKV containing BeH819015 structural proteins was mostly preserved at 48 h post-infection. ZIKV infection can trigger apoptosis in various cell types and cell death occurred at maximum of progeny virus production (Frumence et al., 2016; Huang et al., 2016; Souza et al., 2016). Our previous study showed that ZIKV infection induces BAX-dependent apoptosis in A549 cells (Frumence et al., 2016). A low number of A549[Dual] positive cells for BAX or Caspase 3 activation at 48 h post BR15[MC] or CHIM infection was observed when compared to cells infected with MR766[MC] (Fig. 4B and C). Immunoblot assay using an antibody directed against the 85 kDa-cleaved form of PARP showed that PARP cleavage occurred in A549[Dual] cells infected with MR766[MC] since 24 h post-infection but not with BR15[MC] and CHIM. At 48 h post-infection, PARP cleavage was still moderated for BR15[MC] and CHIM (Fig. 4D). Given that at least 85% of ZIKV-infected A549 cells were positive for expression of E at 48 h p.i. regardless the virus strains tested, the differences in efficiency of PARP cleavage was not related to

a lower percentage of cells infected with ZIKV containing BeH819015 structural proteins (Fig. 3A). Taken together, these results showed that ZIKV-induced apoptosis in A549[Dual] cells is rather delayed in response to viral clones containing BeH819015 structural proteins.

3.4. Expression of ISGs and cytokines in A549 cells infected with viral clones

There is mounting evidence that ZIKV infection leads to the induction of ISGs and expression of pro-inflammatory cytokines in human host cells (Frumence et al., 2016; Hamel et al., 2015, 2017; Quicke et al., 2016). To determine whether viral clones differ in their capacity to activate host-cell responses, we took advantages of A549[Dual] cells which derive from A549 cells by stable integration of two reporter genes: the SEAP and *Lucia* luciferase reporter genes under the transcriptional control of the IFN-ß minimal promoter fused to NF-κB binding sites or an ISG54 minimal promoter in conjunction with ISREs, respectively.

We examined the kinetic of interferon regulatory factor (IRF) pathway activation in ZIKV-infected A549[Dual] cells by monitoring *Lucia* luciferase activity. BR15[MC] and CHIM were poorly efficient at inducing IRF pathway at 24 h and 48 h post-infection when compared to MR766[MC] (Fig. 5A). At 72 h post-infection, activation of the IRF pathway was detected in A549[Dual] cells infected with BR15[MC] or CHIM indicating that significant production of IFN-ß can also occur in response to ZIKV containing BeH819015 structural proteins. This IFN-ß production is even higher than the one measured in MR766-infected cells most probably due to the earlier MR766-mediated cytotoxicity in A549[Dual] cells (Fig. 4). At 24 h post-infection, RT-qPCR analysis showed that IFN-ß gene was up-regulated in response to the three viral clones but to higher level during MR766 infection (Fig. 5B).

We and others reported that ZIKV infection resulted in activation of Interferon-induced proteins with tetratricopeptide repeats (IFIT) family genes (Frumence et al., 2016; Bowen et al., 2017). By RT-qPCR analysis, we showed that ZIKV infection resulted in a minimal (*ISG54/IFIT2* gene) to moderate (*ISG56/IFIT1* gene) expression level of *IFIT* family genes in A549[Dual] cells (Fig. 6A). There were no differences in *ISG54/IFIT2* transcript levels with the three viral clones whereas MR766[MC] and CHIM induced a stronger *ISG56/IFIT1* gene expression than BR15[MC].
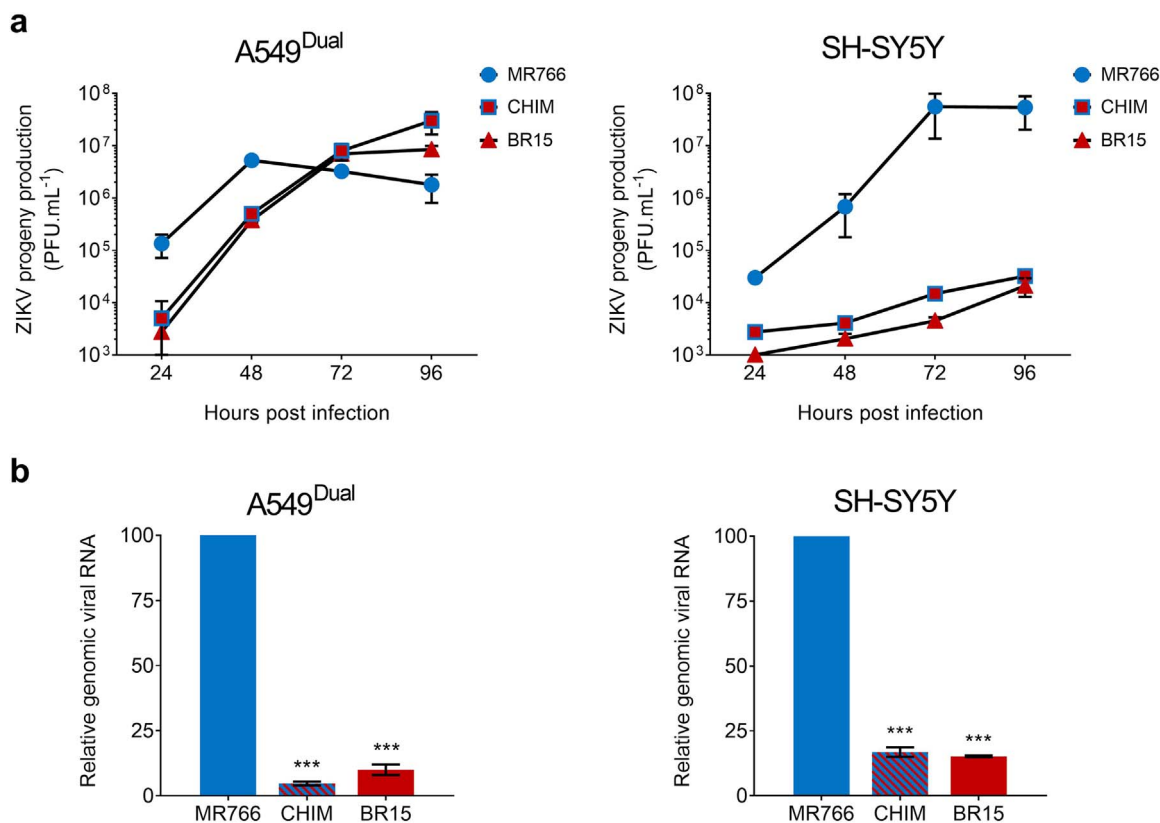
Fig. 2. Analysis of viral growth and virus binding in A549 and SH-SY5Y cells. *In* (A), A549[Dual] cells were infected with MR766[MC], BR15[MC], or CHIM at MOI of 1 and SH-SY5Y cells at MOI of 10. The infectious virus released into the supernatants of infected cells at 24, 48, 72, and 96 h were quantified on Vero cells. The error bars represent the standard deviations of three independent experiments. *In* (B), for virus binding assays, cells were incubated with viral clones at the MOI of 1 (A549[Dual] cells) or 10 (SH-SY5Y cells) for 1 h at 4 °C. The number of virus particles bound to cell surface was measured by RT-qPCR. Values represent the mean and standard deviations of two to four independent experiments.

Thus, infection with ZIKV containing the non-structural proteins of MR766[MC] resulted in stronger induction of *ISG56/IFIT1* gene that has been reported to act as an antagonist of RIG-I-mediated IFN-ß induction (Fensterl and Sen, 2011). This result suggests that the nonstructural protein region is capable of initiating expression of some ISGs in human epithelial cells infected with ZIKV.

We examined the expression pattern of genes commonly involved in the synthesis of pro-inflammatory cytokines by RT-qPCR analysis. At 24 h post-infection, ZIKV infection of A549[Dual] cells resulted in a very weak to no activation of IL-6 and IL-1ß regardless of the viral clone examined (Fig. 6B). This could be corroborated with absence of

detectable NF-κB activity in A549[Dual] cells infected with viral clones (Fig. S1). Thus, infection with MR766[MC] or BR15[MC] did not result in early activation of *IL-6* and *IL-1ß* genes in A549 cells as it has been previously observed with clinical isolate PF-25013-18 of ZIKV (Frumence et al., 2016). At 24 h post-infection, activation of *IL-8* gene was observed in A549[Dual] cells infected with the three viral clones. However, the expression level of *IL-8* gene was significantly higher in response to ZIKV containing nonstructural proteins of MR766 (Fig. 6B). This raises the issue on the role of the nonstructural protein region in the activation of some pro-inflammatory cytokines in human epithelial cells infected with ZIKV.
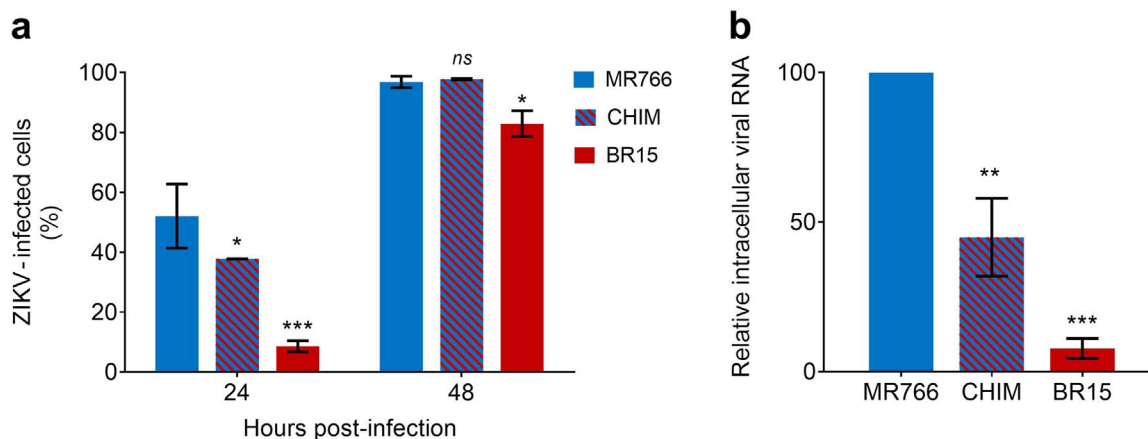
Fig. 3. Viral replication in A549 cells. A549[Dual] cells were infected with MR766[MC], BR15[MC], or CHIM at MOI of 1. *In* (A), the percentages of ZIKV-infected cells at 24 and 48 h were determined by FACS analysis using anti-E mAb 4G2 as primary antibody. The error bars represent the standard deviations of three independent experiments. *In* (B), intracellular viral RNA production was determined by RT-qPCR at 24 h p.i. Values represents the mean and the standard deviations of two independent experiments (n.s. $p > 0.5$, * $p < 0.5$, ** $p < 0.1$).
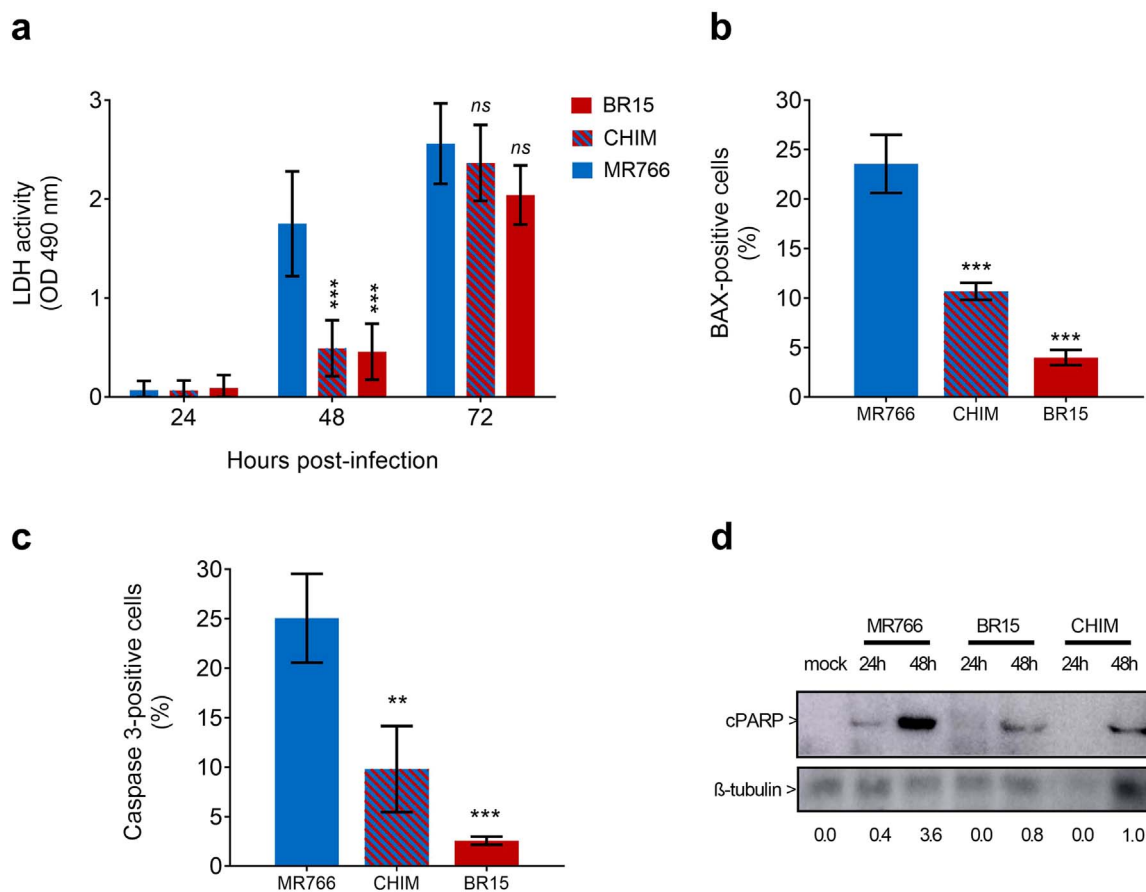
Fig. 4. Kinetics of apoptosis in A549 cells infected with viral clones. A549^{Dual} cells were infected with MR766^{MC}, BR15^{MC}, or CHIM at MOI of 1. *In* (A), LDH activity was measured at 24, 48 and 72 h p.i. Values represents the mean and the standard deviations of three independent experiments (n.s. $p > 0.5$, * $p < 0.5$, ** $p < 0.1$, *** $p < 0.01$). *In* (B), percentage of infected cells immunostained with anti-BAX antibody at 48 h p.i. Values represent the mean and the standard deviations of three independent experiments (*** $p < 0.01$). *In* (C), percentage of infected cells immunostained with anti-caspase 3 antibody at 48 h p.i. Values represent the mean and the standard deviations of three independent experiments (** $p < 0.1$, *** $p < 0.01$). *In* (D), lysate samples of cells infected 24 and 48 h by viral clones were analyzed by immunoblot assay using anti-cleaved PARP antibody. Antibody against β-tubulin served as protein loading control. The head arrows indicate the cleaved form of PARP (cPARP) and β -tubulin. Values below represent cPARP/β-tubulin ratios.

4. Discussion

The association of contemporary ZIKV strains with epidemics and severe forms of disease in humans warrants the need for further characterization of their biological characteristics. The purpose of our study was to better understand the role of the structural proteins in the permissiveness of human cells to ZIKV infection. To this end, two ZIKV molecular clones derived from the Brazilian epidemic strain BeH819015 of Asian lineage and the African historical strain MR766 were compared on their capacity to infect human epithelial A549 and neuroblastoma SH-SY5Y cells. We also generated a chimeric clone derived from MR766 in which C, prM and the first 436 amino acids of E
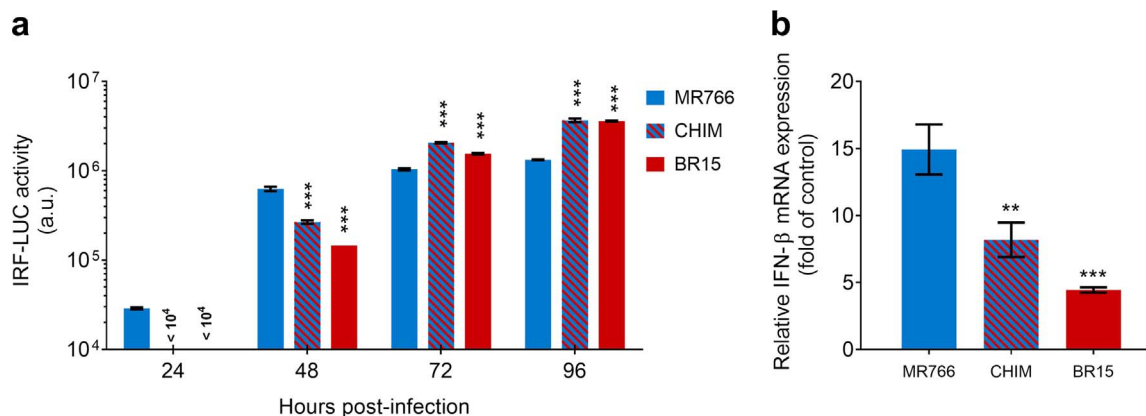
Fig. 5. Activation of IRF and IFN-β pathways in A549 cells infected with viral clones. A549^{Dual} cells were infected with MR766^{MC}, BR15^{MC}, or CHIM at MOI of 1. *In* (A), analysis of IRF pathway activation in response to viral infection. Activity of the secreted *Lucia* luciferase was measured using QUANTI-Luc substrate. Results are expressed as crude data of arbitrary units of luminescence. The results from a representative experiment (n = 3 repeats) are shown (*** $p < 0.01$). *In* (B), production of IFN-β mRNA in response to viral infection. The amount of IFN-β transcripts was determined at 24 h p.i. by RT-qPCR. GAPDH mRNA served as an internal reference. Results are expressed as the fold-induction of IFN-β transcripts in ZIKV-infected cells relative to those in mock-infected cells. Values represent the mean and standard deviations of two independent experiments (** $p < 0.1$, *** $p < 0.01$).

a

ISG54

ISG56

b
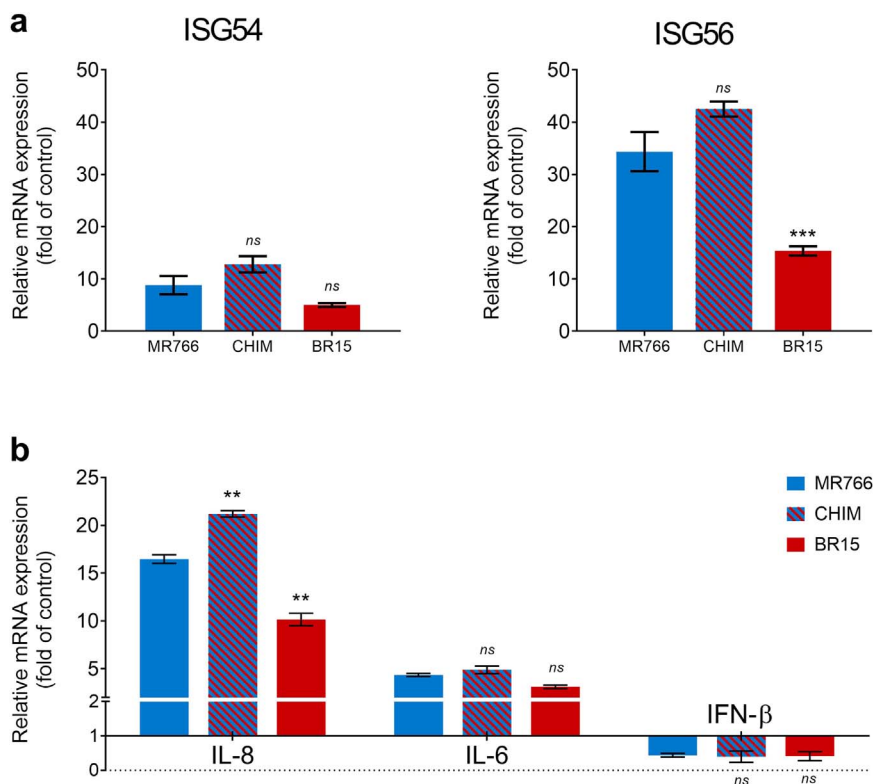
Fig. 6. Activation of ISG54/56 and pro-inflammatory cytokine genes in A549 cells infected with viral clones. A549^{Dual} cells were infected 24 h with MR766^{MC}, BR15^{MC}, or CHIM at MOI of 1. *In* (A) the amounts of ISG54 and ISG56 transcripts were determined by RT-qPCR. GAPDH mRNA served as internal reference. Results are expressed as the fold induction of transcripts relative to those in mock-infected cells. Values represent the mean and standard deviations of triplicates (ns $p > 0.5$, *** $p < 0.01$). *In* (B), the amounts of IL-8, IL-6 and IL-1β transcripts were determined by RT-qPCR. GAPDH mRNA served as internal reference. Results are expressed as the fold induction of transcripts relative to those in mock-infected cells. Values represent the mean and standard deviations of triplicates (ns $p > 0.5$, ** $p < 0.1$).

from MR766 were replaced with those of BeH819015.

Virus binding assay showed that ZIKV containing BeH819015 structural proteins were much less efficient in cell-attachment when compared to MR766. The lower binding capacity of BeH819015 structural proteins was associated with a delay (A549 cells) or severe restriction (SH-SY5Y cells) in viral growth, arguing for an important role of the structural proteins in human epithelial and neuronal cells permissiveness to ZIKV infection. In A549^{Dual} cells, the growth of ZIKV containing BeH819015 structural proteins was deferred resulting in a delayed activation of mitochondrial apoptosis as well as a lower expression level of ISGs and cytokines as compared to African historical strain MR766. We observed that ZIKV containing MR766 nonstructural proteins induced stronger *ISG56/IFIT1* and *IL-8* gene expression in A549^{Dual} cells as compared to the viral clone derived from epidemic BeH819015 strain. It is interesting to speculate that nonstructural protein region of ZIKV has a direct role in the activation of some ISGs and cytokines that might explain differential susceptibility to ZIKV infection.

Binding to cell surface is an absolute pre-requisite for the initiation of viral infection in the host-cell. Attachment and receptor recognition are likely to be processes in which multiples molecules are used in combination or consecutively for virus entry. ZIKV binding assay performed in our study highlighted a critical role of structural proteins in cell attachment. Among the C and prM proteins of MR766 and BeH819015, we found four divergent amino acids in C and ten in prM (Table 2). Flavivirus prM protein, which is essential for viral particle formation, is cleaved by furin protease into "pr" peptide and mature M protein. Several residues of prM have been reported to play an important role in flavivirus replication (Hsieh et al., 2014; Kim et al., 2008; Yoshii et al., 2004, 2012), and N-terminal residues of West Nile prM have been shown essential in virus assembly inside the intracellular membranes (Calvert et al., 2012; Setoh et al., 2015). A lower cleavage efficacy at the pr-M junction could affect the generation of infectious virus particles in promoting the production of prM-containing viruses (Elshuber et al., 2003; Junjhon et al., 2010). We noted that the pr-M junction with the amino acid sequence YGTCH HKKGE

Table 2
Comparative sequence analysis of viral clones.

Viral protein	Amino acid position	Residue MR766^{MC}	Residue BR15^{CprME}-MR766	Residue BR15^{MC}
C	25	N	S	S
	27	L	F	F
	101	R	K	K
	110	I	V	V
prM	3	I	V	V
	17	S	N	N
	21	K	E	E
	26	A	P	P
	31	V	M	M
	35	H	Y	Y
	36	V	I	I
	124	K	R	R
	138	V	A	A
	140	V	A	A
E	120	T	A	A
	152	T	I	I
	156	I	T	T
	158	Y	H	H
	169	V	I	I
	283	K	R	R
	285	F	S	S
	317	V	I	I
	341	I	V	V
	343	V	A	A
	393	D	E	E
	437	V	V	A
	438	F	F	L
	473	V	V	M
	487	T	T	M
	495	M	M	L

Amino acid substitutions in BR15^{MC} and CHIM relative to MR766^{MC} are listed.

ARRSR R/AVTL PSHSS is strictly conserved between ZIKV strains MR766 and BR15 as well as CHIM. Thus, it seems rather unlikely that differences in binding observed among the three virus variants were

correlated with a reduced prM cleavage in ZIKV-infected Vero cells in the course of virus progeny production. On the other hand, the ZIKV prM also contains a single N-glycosylation site at the position prM-70, which is conserved in both historical and epidemic strains. Among the ten amino acid changes between MR766 and BR15 prM proteins, seven are located within the forty N-terminal amino acids (Table 2). Recently, a single Ser to Ala substitution at the position prM-139 protein has been presumed to affect the neuropathogenic properties of ZIKV (Yuan et al., 2017). It remains to be investigated whether the cluster of amino acid changes in the N-terminal region of BeH819015 prM, could contribute to ZIKV strain differences in cell-attachment.

Envelope protein is assumed to bind attachment factors and cellular receptors directing virus particles to the endocytic pathway. ZIKV E protein consists in a four hundred amino acid-long ectodomain which encloses a central ß-barrel shaped domain I (EDI), a finger-like domain II (EDII), and a C-terminal immunoglobulin-like domain III (EDIII) followed by a stem region and two transmembrane domains (Sirohi et al., 2016). Analysis of the chimeric ZIKV MR766 containing BeH819015 structural proteins identified eleven amino acid substitutions that could be potentially involved in the less permissiveness of human host cells to ZIKV strain BeH819015 (Table 2). Three substitutions E-T152I, E-I156T and E-Y158H were identified in EDII. The presence of Thr at position E-156 introduces a potential N-glycosylation site in BeH819015 E protein. The N-glycosylation status of the ZIKV E protein may have a major impact on virus particles assembly and infectivity of epidemic strains as well as virus progeny production (Mossenta et al., 2017; Widman et al., 2017). The role of the three residues at positions E-152, E-156, and E-158 in the biological properties of ZIKV strain BeH819015 requires further analysis. The substitutions E-V317I, E-I341V, E-V343A, and E-D393E were identified in EDIII. It has been shown that ZIKV was impaired in virus particle assembly after the removing of residue E-346 which shortens the extended loop of EDIII (Xie et al., 2017). Whether the four amino acid substitutions mapped into the EDIII are involved in the epidemic ZIKV BeH819015 strain capacity to infect human host cells is an important issue to be investigated.

In conclusion, our study showed differences in host-cell susceptibility to the historical strain MR766 and the epidemic strain BeH819015 and highlighted a potential role of the structural proteins in the permissiveness of human epithelial and neuronal cells to ZIKV infection. It was striking to observe that the growth of Asian epidemic strain BeH819015 was poorly efficient in neuroblastoma SH-SY5Y cells whereas infection with African historical strain MR766 was highly productive. The attenuated replication of BeH819015 in human neuronal cells was associated to a minimal loss of cell viability on at least one week (data not shown and Fig. S2). The greater capacity of epidemic strains of ZIKV to initiate persistent infection in specialized human cells is a critical issue that must be urgently investigated. (Bhatnagar et al., 2017; Epelboin et al., 2017; Mladinich et al., 2017).

It is not well understood whether ZIKV strains of African and Asian lineages use the same factors for attachment to cell surface with different affinities, or authorize distinct molecules for endocytosis of virus particles. To date, little is known on attachment factors and entry receptors that contribute to the permissiveness of SH-SY5Y cells to ZIKV. It has been reported that the TIM-receptor AXL binds ZIKV via Gas 6 and mediates viral entry in neural cells of human origin (Meertens et al., 2017). Among the diverging residues identified between MR766 and BeH819015 structural proteins, it is therefore urgent to determine which ones could contribute to the permissiveness of human neural cells to ZIKV infection.

Acknowledgements

Appendix A. Supplementary material

Supplementary data associated with this article can be found in the online version at http://dx.doi.org/10.1016/j.virol.2017.12.003.

References

Alcendor, D.J., 2017. Zika virus infection of the human glomerular cells: implications for viral reservoirs and renal pathogenesis. J. Infect. Dis. 216, 162–171. http://dx.doi.org/10.1093/infdis/jix171.

Atieh, T., Baronti, C., de Lamballerie, X., Nougairède, A., 2016. Simple reverse genetics systems for Asian and African Zika viruses. Sci. Rep. 6, 39384. http://dx.doi.org/10.1038/srep39384.

Bhatnagar, J., Rabeneck, D.B., Martines, R.B., Reagan-Steiner, S., Ermias, Y., Estetter, L.B.C., Suzuki, T., Ritter, J., Keating, M.K., Hale, G., Gary, J., Muehlenbachs, A., Lambert, A., Lanciotti, R., Oduyebo, T., Meaney-Delman, D., Bolaños, F., Saad, E.A.P., Shieh, W.-J., Zaki, S.R., 2017. Zika virus RNA replication and persistence in brain and placental tissue. Emerg. Infect. Dis. 23, 405–414. http://dx.doi.org/10.3201/eid2303.161499.

Calvert, A.E., Huang, C.Y.-H., Blair, C.D., Roehrig, J.T., 2012. Mutations in the West Nile prM protein affect VLP and virion secretion in vitro. Virology 433, 35–44. http://dx.doi.org/10.1016/j.virol.2012.07.011.

Cao-Lormeau, V.-M., Blake, A., Mons, S., Lastère, S., Roche, C., Vanhomwegen, J., Dub, T., Baudouin, L., Teissier, A., Larre, P., Vial, A.-L., Decam, C., Choumet, V., Halstead, S.K., Willison, H.J., Musset, L., Manuguerra, J.-C., Despres, P., Fournier, E., Mallet, H.-P., Musso, D., Fontanet, A., Neil, J., Ghawché, F., 2016. Guillain-Barré Syndrome outbreak associated with Zika virus infection in French Polynesia: a case-control study. Lancet 387, 1531–1539. http://dx.doi.org/10.1016/S0140-6736(16)00562-6.

Cao-Lormeau, V.-M., Roche, C., Teissier, A., Robin, E., Berry, A.-L., Mallet, H.-P., Sall, A.A., Musso, D., 2014. Zika virus, French polynesia, South pacific, 2013. Emerg. Infect. Dis. 20, 1085–1086. http://dx.doi.org/10.3201/eid2006.140138.

Cugola, F.R., Fernandes, I.R., Russo, F.B., Freitas, B.C., Dias, J.L.M., Guimarães, K.P., Benazzato, C., Almeida, N., Pignatari, G.C., Romero, S., Polonio, C.M., Cunha, I., Freitas, C.L., Brandão, W.N., Rossato, C., Andrade, D.G., Faria, D., de, P., Garcez, A.T., Buchpigel, C.A., Braconi, C.T., Mendes, E., Sall, A.A., Zanotto, P.M., de, A., Peron, J.P.S., Muotri, A.R., Beltrão-Braga, P.C.B., 2016. The Brazilian Zika virus strain causes birth defects in experimental models. Nature 534, 267–271. http://dx.doi.org/10.1038/nature18296.

Dick, G.W.A., Kitchen, S.F., Haddow, A.J., 1952. Zika Virus (I). Isolations and serological specificity. Trans. R. Soc. Trop. Med. Hyg. 46, 509–520. http://dx.doi.org/10.1016/0035-9203(52)90042-4.

D'Ortenzio, E., Matheron, S., Yazdanpanah, Y., de Lamballerie, X., Hubert, B., Piorkowski, G., Maquart, M., Descamps, D., Damond, F., Leparc-Goffart, I., 2016. Evidence of sexual transmission of Zika virus. N. Engl. J. Med. 374, 2195–2198. http://dx.doi.org/10.1056/NEJMc1604449.

Duffy, M.R., Chen, T.-H., Hancock, W.T., Powers, A.M., Kool, J.L., Lanciotti, R.S., Pretrick, M., Marfel, M., Holzbauer, S., Dubray, C., Guillaumot, L., Griggs, A., Bel, M., Lambert, A.J., Laven, J., Kosoy, O., Panella, A., Biggerstaff, B.J., Fischer, M., Hayes, E.B., 2009. Zika virus outbreak on Yap Island, Federated States of Micronesia. N. Engl. J. Med. 360, 2536–2543. http://dx.doi.org/10.1056/NEJMoa0805715.

Elshuber, S., Allison, S.L., Heinz, F.X., Mandl, C.W., 2003. Cleavage of protein prM is necessary for infection of BHK-21 cells by tick-borne encephalitis virus. J. Gen. Virol. 84, 183–191. http://dx.doi.org/10.1099/vir.0.18723-0.

Epelboin, S., Dulioust, E., Epelboin, L., Benachi, A., Merlet, F., Patrat, C., 2017. Zika virus and reproduction: facts, questions and current management. Hum. Reprod. Update 23, 629–645. http://dx.doi.org/10.1093/humupd/dmx024.

Faria, N.R., Azevedo, R., do, S., da, S., Kraemer, M.U.G., Souza, R., Cunha, M.S., Hill, S.C., Thézé, J., Bonsall, M.B., Bowden, T.A., Rissanen, I., Rocco, I.M., Nogueira, J.S., Maeda, A.Y., Vasami, F.G., da, S., Macedo, F.L., de, L., Suzuki, A., Rodrigues, S.G., Cruz, A.C.R., Nunes, B.T., Medeiros, D.B., de, A., Rodrigues, D.S.G., Queiroz, A.L.N., da Silva, E.V.P., Henriques, D.F., da Rosa, E.S.T., de Oliveira, C.S., Martins, L.C., Vasconcelos, H.B., Casseb, L.M.N., Simith, D., de, B., Messina, J.P., Abade, L., Lourenço, J., Alcantara, L.C.J., de Lima, M.M., Giovanetti, M., Hay, S.I., de Oliveira, R.S., Lemos, P., da, S., de Oliveira, L.F., de Lima, C.P.S., da Silva, S.P., de Vasconcelos, J.M., Franco, L., Cardoso, J.F., Vianez-Júnior, J.L., da, S.G., Mir, D., Bello, G., Delatorre, E., Khan, K., Creatore, M., Coelho, G.E., de Oliveira, W.K., Tesh, R., Pybus, O.G., Nunes, M.R.T., Vasconcelos, P.F.C., 2016. Zika virus in the Americas: early epidemiological and genetic findings. Science 352, 345–349. http://dx.doi.org/10.1126/science.aaf5036.

Fensterl, V., Sen, G.C., 2011. The ISG56/IFIT1 gene family. J. Interferon Cytokine Res. 31, 71–78. http://dx.doi.org/10.1089/jir.2010.0101.

Frumence, E., Roche, M., Krejbich-Trotot, P., El-Kalamouni, C., Nativel, B., Rondeau, P., Missé, D., Gadea, G., Viranaicken, W., Desprès, P., 2016. The South Pacific epidemic strain of Zika virus replicates efficiently in human epithelial A549 cells leading to IFN-β production and apoptosis induction. Virology 493, 217–226. http://dx.doi.org/10.1016/j.virol.2016.03.006.

Gadea, G., Bos, S., Krejbich-Trotot, P., Clain, E., Viranaicken, W., El-Kalamouni, C., Mavingui, P., Desprès, P., 2016. A robust method for the rapid generation of recombinant Zika virus expressing the GFP reporter gene. Virology 497, 157–162. http://dx.doi.org/10.1016/j.virol.2016.07.015.

Gatherer, D., Kohl, A., 2016. Zika virus: a previously slow pandemic spreads rapidly through the Americas. J. Gen. Virol. 97, 269–273. http://dx.doi.org/10.1099/jgv.0.000381.

Giovanetti, M., Milano, T., Alcantara, L.C., Carcangiu, L., Cella, E., Lai, A., Lo Presti, A., Pascarella, S., Zehender, G., Angeletti, S., Ciccozzi, M., 2016. Zika virus spreading in South America: evolutionary analysis of emerging neutralizing resistant Phe279Ser strains. Asian Pac. J. Trop. Med. 9, 445–452. http://dx.doi.org/10.1016/j.apjtm.2016.03.028.

Haddow, A.D., Schuh, A.J., Yasuda, C.Y., Kasper, M.R., Heang, V., Huy, R., Guzman, H., Tesh, R.B., Weaver, S.C., 2012. Genetic characterization of Zika virus strains: geographic expansion of the Asian lineage. PLoS Negl. Trop. Dis. 6, e1477. http://dx.doi.org/10.1371/journal.pntd.0001477.

Hamel, R., Dejarnac, O., Wichit, S., Ekchariyawat, P., Neyret, A., Luplertlop, N., Perera-Lecoin, M., Surasombatpattana, P., Talignani, L., Thomas, F., Cao-Lormeau, V.-M., Choumet, V., Briant, L., Desprès, P., Amara, A., Yssel, H., Missé, D., 2015. Biology of Zika Virus infection in human skin cells. J. Virol. 89, 8880–8896. http://dx.doi.org/10.1128/JVI.00354-15.

Hamel, R., Ferraris, P., Wichit, S., Diop, F., Talignani, L., Pompon, J., Garcia, D., Liégeois, F., Sall, A.A., Yssel, H., Missé, D., 2017. African and Asian Zika virus strains differentially induce early antiviral responses in primary human astrocytes. Infect. Genet. Evol. 49, 134–137. http://dx.doi.org/10.1016/j.meegid.2017.01.015.

Hsieh, S.-C., Wu, Y.-C., Zou, G., Nerurkar, V.R., Shi, P.-Y., Wang, W.-K., 2014. Highly conserved residues in the helical domain of dengue virus type 1 precursor membrane protein are involved in assembly, precursor membrane (prM) protein cleavage, and entry. J. Biol. Chem. 289, 33149–33160. http://dx.doi.org/10.1074/jbc.M114.610428.

Huang, W.-C., Abraham, R., Shim, B.-S., Choe, H., Page, D.T., 2016. Zika virus infection during the period of maximal brain growth causes microcephaly and corticospinal neuron apoptosis in wild type mice. Sci. Rep. 6, 34793. http://dx.doi.org/10.1038/srep34793.

Junjhon, J., Edwards, T.J., Utaipat, U., Bowman, V.D., Holdaway, H.A., Zhang, W., Keelapang, P., Puttikhunt, C., Perera, R., Chipman, P.R., Kasinrerk, W., Malasit, P., Kuhn, R.J., Sittisombut, N., 2010. Influence of pr-M cleavage on the heterogeneity of extracellular dengue virus particles. J. Virol. 84, 8353–8358. http://dx.doi.org/10.1128/JVI.00696-10.

Kim, J.-M., Yun, S.-I., Song, B.-H., Hahn, Y.-S., Lee, C.-H., Oh, H.-W., Lee, Y.-M., 2008. A single N-linked glycosylation site in the Japanese encephalitis virus prM protein is critical for cell type-specific prM protein biogenesis, virus particle release, and pathogenicity in mice. J. Virol. 82, 7846–7862. http://dx.doi.org/10.1128/JVI.00789-08.

Meertens, L., Labeau, A., Dejarnac, O., Cipriani, S., Sinigaglia, L., Bonnet-Madin, L., Le Charpentier, T., Hafirassou, M.L., Zamborlini, A., Cao-Lormeau, V.-M., Coulpier, M., Missé, D., Jouvenet, N., Tabibiazar, R., Gressens, P., Schwartz, O., Amara, A., 2017. Axl mediates ZIKA virus entry in human glial cells and modulates innate immune responses. Cell Rep. 18, 324–333. http://dx.doi.org/10.1016/j.celrep.2016.12.045.

Merfeld, E., Ben-Avi, L., Kennon, M., Cerveny, K.L., 2017. Potential mechanisms of Zika-linked microcephaly. Wiley Interdiscip. Rev. Dev. Biol. http://dx.doi.org/10.1002/wdev.273.

Mladinich, M.C., Schwedes, J., Mackow, E.R., 2017. Zika virus persistently infects and is basolaterally released from primary human brain microvascular endothelial cells. mBio 8. http://dx.doi.org/10.1128/mBio.00952-17.

Mossenta, M., Marchese, S., Poggianella, M., Slon Campos, J.L., Burrone, O.R., 2017. Role of N-glycosylation on Zika virus E protein secretion, viral assembly and infectivity. Biochem. Biophys. Res. Commun. http://dx.doi.org/10.1016/j.bbrc.2017.01.022.

Motta, I.J.F., Spencer, B.R., Cordeiro da Silva, S.G., Arruda, M.B., Dobbin, J.A., Gonzaga, Y.B.M., Arcuri, I.P., Tavares, R.C.B.S., Atta, E.H., Fernandes, R.F.M., Costa, D.A., Ribeiro, L.J., Limonte, F., Higa, L.M., Voloch, C.M., Brindeiro, R.M., Tanuri, A., Ferreira, O.C., 2016. Evidence for transmission of Zika virus by platelet transfusion. N. Engl. J. Med. 375, 1101–1103. http://dx.doi.org/10.1056/NEJMc1607262.

Musso, D., Stramer, S.L., 2016. AABB Transfusion-Transmitted Diseases Committee, Busch, M.P., International Society of Blood Transfusion Working Party on Transfusion-Transmitted Infectious Diseases. Zika virus: a new challenge for blood transfusion. Lancet. 387, 1993–1994. ⟨http://dx.doi.org/10.1016/S0140-6736(16)30428-7⟩.

Nativel, B., Marimoutou, M., Thon-Hon, V.G., Gunasekaran, M.K., Andries, J., Stanislas, G., Planesse, C., Da Silva, C.R., Césari, M., Iwema, T., Gasque, P., Viranaicken, W.,

2013. Soluble HMGB1 is a novel adipokine stimulating IL-6 secretion through RAGE receptor in SW872 preadipocyte cell line: contribution to chronic inflammation in fat tissue. PLoS One 8, e76039. http://dx.doi.org/10.1371/journal.pone.0076039.

Pagani, I., Ghezzi, S., Ulisse, A., Rubio, A., Turrini, F., Garavaglia, E., Candiani, M., Castilletti, C., Ippolito, G., Poli, G., Broccoli, V., Panina-Bordignon, P., Vicenzi, E., 2017. Human endometrial stromal cells are highly permissive to productive infection by Zika virus. Sci. Rep. 7, 44286. http://dx.doi.org/10.1038/srep44286.

Parra, B., Lizarazo, J., Jiménez-Arango, J.A., Zea-Vera, A.F., González-Manrique, G., Vargas, J., Angarita, J.A., Zuñiga, J., Lopez-Gonzalez, R., Beltran, C.L., Rizcala, K.H., Morales, M.T., Pacheco, O., Ospina, M.L., Kumar, A., Cornblath, D.R., Muñoz, L.S., Osorio, L., Barreras, P., Pardo, C.A., 2016. Guillain-Barré syndrome associated with Zika virus infection in Colombia. N. Engl. J. Med. 375, 1513–1523. http://dx.doi.org/10.1056/NEJMoa1605564.

Quicke, K.M., Bowen, J.R., Johnson, E.L., McDonald, C.E., Ma, H., O'Neal, J.T., Rajakumar, A., Wrammert, J., Rimawi, B.H., Pulendran, B., Schinazi, R.F., Chakraborty, R., Suthar, M.S., 2016. Zika virus infects human placental macrophages. Cell Host Microbe 20, 83–90. http://dx.doi.org/10.1016/j.chom.2016.05.015.

Setoh, Y.X., Tan, C.S.E., Prow, N.A., Hobson-Peters, J., Young, P.R., Khromykh, A.A., Hall, R.A., 2015. The I22V and L72S substitutions in West Nile virus prM protein promote enhanced prM/E heterodimerisation and nucleocapsid incorporation. Virol. J. 12, 72. http://dx.doi.org/10.1186/s12985-015-0303-7.

Sheridan, M.A., Yunusov, D., Balaraman, V., Alexenko, A.P., Yabe, S., Verjovski-Almeida, S., Schust, D.J., Franz, A.W., Sadovsky, Y., Ezashi, T., Roberts, R.M., 2017. Vulnerability of primitive human placental trophoblast to Zika virus. Proc. Natl. Acad. Sci. USA 114, E1587–E1596. http://dx.doi.org/10.1073/pnas.1616097114.

Simonin, Y., Loustalot, F., Desmetz, C., Foulongne, V., Constant, O., Fournier-Wirth, C., Leon, F., Molès, J.-P., Goubaud, A., Lemaitre, J.-M., Maquart, M., Leparc-Goffart, I., Briant, L., Nagot, N., Van de Perre, P., Salinas, S., 2016. Zika virus strains potentially display different infectious profiles in human neural cells. EBioMedicine 12, 161–169. http://dx.doi.org/10.1016/j.ebiom.2016.09.020.

Sirohi, D., Chen, Z., Sun, L., Klose, T., Pierson, T.C., Rossmann, M.G., Kuhn, R.J., 2016. The 3.8 Å resolution cryo-EM structure of Zika virus. Science 352, 467–470. http://dx.doi.org/10.1126/science.aaf5316.

Souza, B.S.F., Sampaio, G.L.A., Pereira, C.S., Campos, G.S., Sardi, S.I., Freitas, L.A.R., Figueira, C.P., Paredes, B.D., Nonaka, C.K.V., Azevedo, C.M., Rocha, V.P.C., Bandeira, A.C., Mendez-Otero, R., Dos Santos, R.R., Soares, M.B.P., 2016. Zika virus infection induces mitosis abnormalities and apoptotic cell death of human neural progenitor cells. Sci. Rep. 6, 39775. http://dx.doi.org/10.1038/srep39775.

Tripathi, S., Balasubramaniam, V.R.M.T., Brown, J.A., Mena, I., Grant, A., Bardina, S.V., Maringer, K., Schwarz, M.C., Maestre, A.M., Sourisseau, M., Albrecht, R.A., Krammer, F., Evans, M.J., Fernandez-Sesma, A., Lim, J.K., García-Sastre, A., 2017. A novel Zika virus mouse model reveals strain specific differences in virus pathogenesis and host inflammatory immune responses. PLoS Pathog. 13, e1006258. http://dx.doi.org/10.1371/journal.ppat.1006258.

Viranaicken, W., Gasmi, L., Chaumet, A., Durieux, C., Georget, V., Denoulet, P., Larcher, J.-C., 2011. L-Ilf3 and L-NF90 traffic to the nucleolus granular component: alternatively-spliced exon 3 encodes a nucleolar localization motif. PLoS One 6, e22296. http://dx.doi.org/10.1371/journal.pone.0022296.

Widman, D.G., Young, E., Yount, B.L., Plante, K.S., Gallichotte, E.N., Carbaugh, D.L., Peck, K.M., Plante, J., Swanstrom, J., Heise, M.T., Lazear, H.M., Baric, R.S., 2017. A reverse genetics platform that spans the Zika virus family tree. mBio 8. http://dx.doi.org/10.1128/mBio.02014-16.

Xie, X., Yang, Y., Muruato, A.E., Zou, J., Shan, C., Nunes, B.T.D., Medeiros, D.B.A., Vasconcelos, P.F.C., Weaver, S.C., Rossi, S.L., Shi, P.-Y., 2017. Understanding Zika virus stability and developing a chimeric vaccine through functional analysis. mBio 8. http://dx.doi.org/10.1128/mBio.02134-16.

Yoshii, K., Igarashi, M., Ichii, O., Yokozawa, K., Ito, K., Kariwa, H., Takashima, I., 2012. A conserved region in the prM protein is a critical determinant in the assembly of flavivirus particles. J. Gen. Virol. 93, 27–38. http://dx.doi.org/10.1099/vir.0.035964-0.

Yoshii, K., Konno, A., Goto, A., Nio, J., Obara, M., Ueki, T., Hayasaka, D., Mizutani, T., Kariwa, H., Takashima, I., 2004. Single point mutation in tick-borne encephalitis virus prM protein induces a reduction of virus particle secretion. J. Gen. Virol. 85, 3049–3058. http://dx.doi.org/10.1099/vir.0.80169-0.

Yuan, L., Huang, X.-Y., Liu, Z.-Y., Zhang, F., Zhu, X.-L., Yu, J.-Y., Ji, X., Xu, Y.-P., Li, G., Li, C., Wang, H.-J., Deng, Y.-Q., Wu, M., Cheng, M.-L., Ye, Q., Xie, D.-Y., Li, X.-F., Wang, X., Shi, W., Hu, B., Shi, P.-Y., Xu, Z., Qin, C.-F., 2017. A single mutation in the prM protein of Zika virus contributes to fetal microcephaly. Science eaam7120. http://dx.doi.org/10.1126/science.aam7120.